Photoluminescence and photoluminescence excitation studies of lateral size effects in $Zn_{1-x}Mn_xSe$/ZnSe quantum disc samples of different radii

P. J. Klar, D. Wolverson and J. J. Davies
School of Physics, University of East Anglia
Norwich NR4 7TJ, United Kingdom
W. Heimbrodt and M. Happ
Institut für Physik, Humboldt-Universität zu Berlin
Invalidenstraße 110, D-10115 Berlin, Germany
T. Henning
Applied Solid State Physics, University of Göteborg and
Chalmers University of Technology, S-41296 Göteborg, Sweden

cond-mat/9803208

Abstract

Quantum disc structures (with diameters of 200 nm and 100 nm) were prepared from a $Zn_{0.72}Mn_{0.28}Se$/ZnSe single quantum well structure by electron beam lithography followed by an etching procedure which combined dry and wet etching techniques. The quantum disc structures and the parent structure were studied by photoluminescence and photoluminescence excitation spectroscopy. For the light-hole excitons in the quantum well region, shifts of the energy positions are observed following fabrication of the discs, confirming that strain relaxation occurs in the pillars. The light-hole exciton lines also sharpen following disc fabrication: this is due to an interplay between strain effects (related to dislocations) and the lateral size of the discs. A further consequence of the small lateral sizes of the discs is that the intensity of the donor-bound exciton emission from the disc is found to decrease with the disc radius. These size-related effects occur before the disc radius is reduced to dimensions necessary for lateral quantum confinement to occur but will remain important when the discs are made small enough to be considered as quantum dots.

1 Introduction

The development of etching methods for II-VI semiconductor heterostructures which allow a further reduction of dimensionality towards quantum dots (Q-dots) and quantum wires (Q-wires) is currently of interest. So far, three different etching techniques have been used: ion beam etching (IBE) [1, 2], reactive ion etching (RIE) [3] and wet-chemical etching (WCE) [4, 5]. The anisotropy of dry etching processes such as RIE or IBE allows the fabrication of patterns with a small spacing and of considerable etch depth. However, nanostructures fabricated using IBE show considerable surface damage (up to depths of about 30 nm) [6]. In contrast, the surface damage induced by WCE is small: recently, the preparation by this method of high-quality $Zn_{1-x}Cd_xSe$/ZnSe Q-dot and Q-wire structures down to lateral sizes of 20 nm with a high photoluminescence (PL) quantum efficiency was reported and, in that work, the observation of quantum confinement effects via PL was possible [5]. The major disadvantage of WCE is that, because of the mainly isotropic etch process, only low-density patterns of Q-dots and Q-wires can be obtained. From the point of view of future applications, it is desirable to fabricate large areas of high-quality nanostructures with high-density patterns by methods which combine the advantages of dry and wet-chemical etching. Attempts in this direction have been made by Gurevich et al., who combined RIE and WCE [6] and by Gourgon et al., who used anodic oxidation after IBE to remove the damaged surface layer [7].

We report here on an etching technique which combines Ar^{2+} IBE and WCE. Using this novel combination of techniques, we prepared large areas (3.2 mm × 3.2 mm) of $Zn_{0.72}Mn_{0.28}Se$/ZnSe pillars containing single quantum wells of uniform diameters of either 200 nm or 100 nm, with area densities respectively of 1:4 and 1:16 in the pattern. The lateral dimensions of the quantum layers are too large for lateral quantum confinement effects to be important and we therefore refer to the structures as quantum discs (rather than quantum dots). In studying these discs, we find that there are significant size effects of a *non-quantum* nature that must be taken into account and which must be fully elucidated if the behaviour of quantum dots themselves is also to be understood.

Nanostructures from the $Zn_{1-x}Mn_xSe$/ZnSe system are of interest not only because of their close relation to the wide-bandgap II-VI materials used in blue-green optoelectronic devices, but also because of the variety of additional effects that arise from the unique magnetic properties of dilute magnetic semiconductors (DMS). Although the effects of magnetic field are not explicitly part of the present work, we shall make use of spectral changes induced by magnetic fields in order to identify certain transitions. The usefulness of magneto-optical experiments on DMS quantum structures to address problems of nanofabrication as well as fundamental physical problems has been demonstrated elsewhere [8].

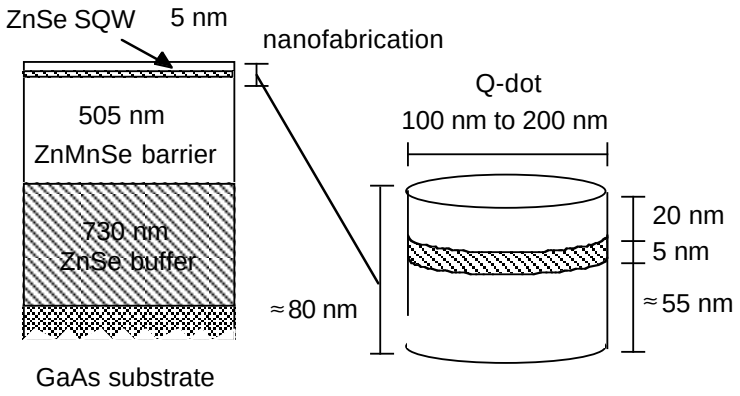

Figure 1: Schematic diagrams of the $Zn_{0.72}Mn_{0.28}Se$/ZnSe single quantum well structure (left) and of a pillar with quantum disc (right). The pillars are etched only to a depth of about 80 nm from the surface into the sample in the nanofabrication process. The layer thicknesses of the parent structure and the dimensions of the pillars are indicated.

2 Sample preparation

The $Zn_{0.72}Mn_{0.28}Se$/ZnSe single quantum well (SQW) structure used for the nanofabrication of the Q-dots was grown on an almost exactly (100) oriented GaAs substrate in a DCA 350 MBE system equipped with effusion cells for Zn, Cd, Mn and Se. The growth was carried out in a phase-locked epitaxial mode based on RHEED [9]. The SQW structure was deposited on a ZnSe buffer layer of 730 nm thickness and consisted of a 505 nm thick barrier layer followed by the quantum well layer of 5.1 nm and a 20 nm barrier as a capping layer (figure 1).

The nanofabrication process of the Q-dot samples was based on the eight step technique described in detail earlier [2]. Only small modifications were made for the preparation of the 200 nm Q-dot sample. The dose in the electron beam lithography process was reduced to 205 $\mu C/cm^2$ and etching was carried out by Ar^{2+} IBE through the quantum well into the lower lying barrier to a depth of about 80 nm. The first fabrication steps for the 100 nm Q-dot sample were the same as for the 200 nm Q-dot sample. However, to reduce the diameter of the Q-dots to 100 nm, wet-chemical etching was used as an additional step before the removal of the Ti-protection mask. The etchant used was a solution of bromine and ethylene glycol with a solution ratio of Br_2:$HOCH_2CH_2OH$ of 2:1000 [4]. Figure 2 shows an SEM image of the 100 nm Q-dot sample before the removal of the Ti-protection mask.

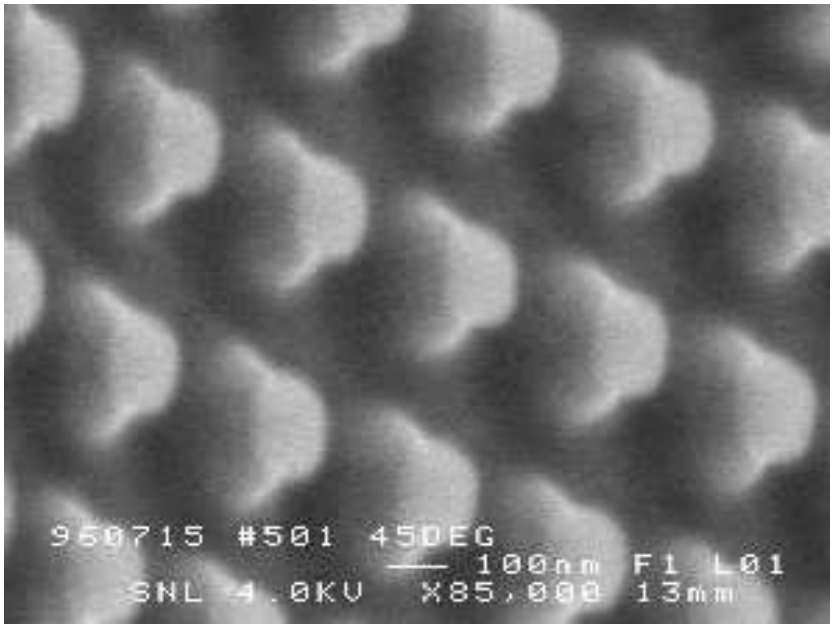

Figure 2: Image of the 100 nm Q-disc pillars taken by scanning electron microscopy after wet-chemical etching and before removal of the titanium protection mask. The scale of the figure is indicated by the horizontal bar.

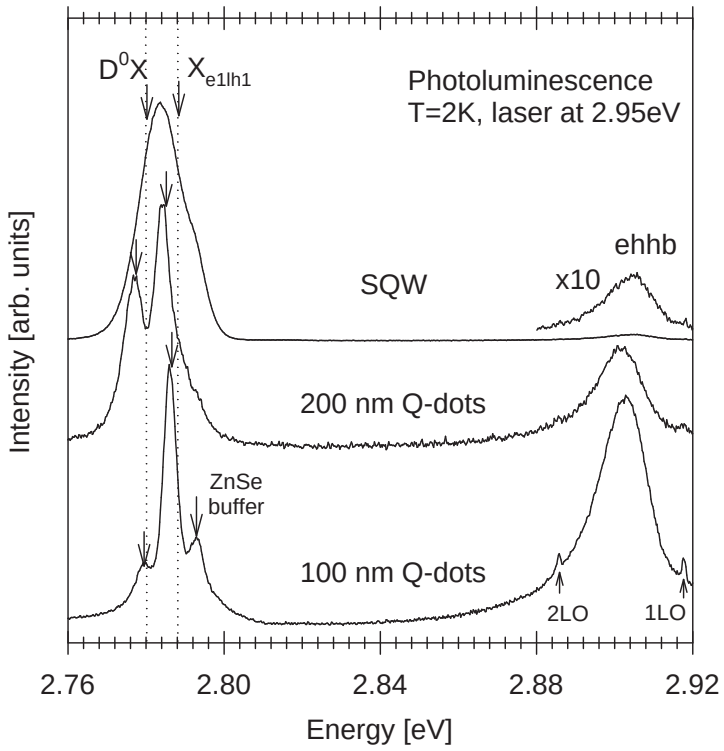

Figure 3: Photoluminescence spectra of the parent $Zn_{0.72}Mn_{0.28}Se/ZnSe$ structure and the 200 nm and 100 nm Q-disc samples. The spectra are shifted vertically for clarity. D^0X and X_{e1lh1} denote the donor-bound and the free exciton emission bands respectively from the quantum well layer in each specimen and, in the lowest spectum, two bands arising from Raman scattering of phonons are also indicated (1LO and 2LO).

3 Results and Discussion

The PL and the photoluminescence excitation (PLE) experiments were carried out with the sample in liquid helium at 2 K. A tunable dye laser (Stilbene 3) pumped by the UV emission of an Ar^{2+} laser was used as excitation source and a single grating spectrometer equipped with a charge-coupled device detector was used for detection. The PL spectra were recorded directly, whereas the PLE spectra were derived from sets of complete PL spectra taken at different finely-spaced excitation energies. The magneto-optical measurements were carried out by means of a superconducting magnet system. Spectra were taken in the Faraday configuration (with the layer plane of the specimens normal to the magnetic field) for σ^+ and σ^- circularly polarised light at magnetic fields up to 7 Tesla.

Figure 3 depicts a comparison of the PL spectra of the three specimens. All the spectra were obtained with the energy of the excitation laser light above the bandgap of the $Zn_{0.72}Mn_{0.28}Se$ barrier. At the right-hand end of each spectrum a signal appears at about 2.905 eV: the shift in the position of this signal when a magnetic field is applied enables it to be identified as being due to a heavy-hole barrier (ehhb) exciton (the large shift in energy of such transitions is caused by the so-called giant enhancement of the applied magnetic field by the exchange interaction between the charge carriers and the magnetic ions in the dilute magnetic material). In the left-hand part of the PL spectrum from the quantum well layer (upper spectrum) there appears a signal made up of two overlapping bands. Again, when a magnetic field is applied, both these bands shift in energy and can be attributed to recombination transitions in the quantum well involving the free light-hole exciton, denoted by X_{e1lh1}, and, at slightly lower energy, a donor-bound exciton, denoted as D^0X (the field induced shifts in these transitions are due to penetration of the well wavefunctions into the barrier regions, which are magnetic).

When the structures are etched to form the quantum discs, there are no significant changes in the emission from the $Zn_{0.72}Mn_{0.28}Se$ barriers (the successive increases in intensity are due simply to the increase, through uncovering, of the area of the barrier directly exposed to the excitation). In contrast, there are several interesting changes in the PL from the ZnSe well. For the 200 nm discs, the D^0X and X_{e1lh1} lines are both shifted towards lower energy by about 4 meV relative to the corresponding lines in the unetched material and are sharpened. When the disc radius is reduced to 100 nm, the exciton lines remain sharp and shift partly (by about 2 meV), but not completely, back towards their positions in the original layer. A further noticeable feature is the marked decrease in the intensity of the D^0X emission relative to that of the X_{e1lh1} in going from the original layer to the 200 nm Q-discs and then to those of 100 nm diameter, for which the D^0X emission has almost disappeared. The emission band at 2.792 eV in the PL spectrum of the 100 nm Q-dot sample originates from the ZnSe buffer, as is readily confirmed by its lack of sensitivity to an applied magnetic field.

Further information about the excitonic states of the samples can be obtained from the PLE spectra (which were taken by monitoring the low energy side of the quantum well PL). Before we compare the three samples, it is useful to look at the evolution of the PLE spectra with magnetic field, which helps to identify the peaks unambiguously. In figure 4, the excitation spectra of the 200 nm Q-discs are depicted as an example. The sharp lines are due to one- and two-phonon LO phonon Raman scattering and do not move in an external magnetic field. There are also no shifts of the bands lying somewhat below 2.8 eV and these are attributed, therefore, to the ZnSe buffer layer. However, a clearly observable shift is seen for both the remaining bands, which are therefore ascribed to the e1lh1 and e1hh1 well states. The shift with magnetic field is caused by the exchange interaction between the well excitons and the localised Mn spins in the barrier. Shifts of about 4 meV and 13 meV to higher energies in case of σ^- circularly polarised light are typically observed for the e1lh1 and e1hh1 excitons respectively in ZnSe wells of width about 5 nm between $Zn_{0.72}Mn_{0.28}Se$ barriers.

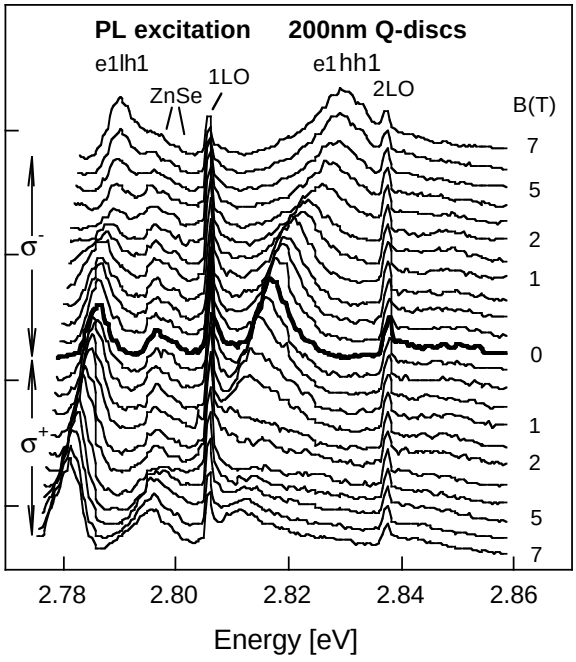

Figure 4: Photoluminescence excitation spectra of the 200 nm Q-discs sample at magnetic fields from 0 to 7 Tesla in the Faraday configuration with σ^- and σ^+ circularly polarised light. The magnetic field step size was 0.25 T from 0 to 1 T, and 1 T beyond that; the zero-field spectrum is indicated by the heavier line.

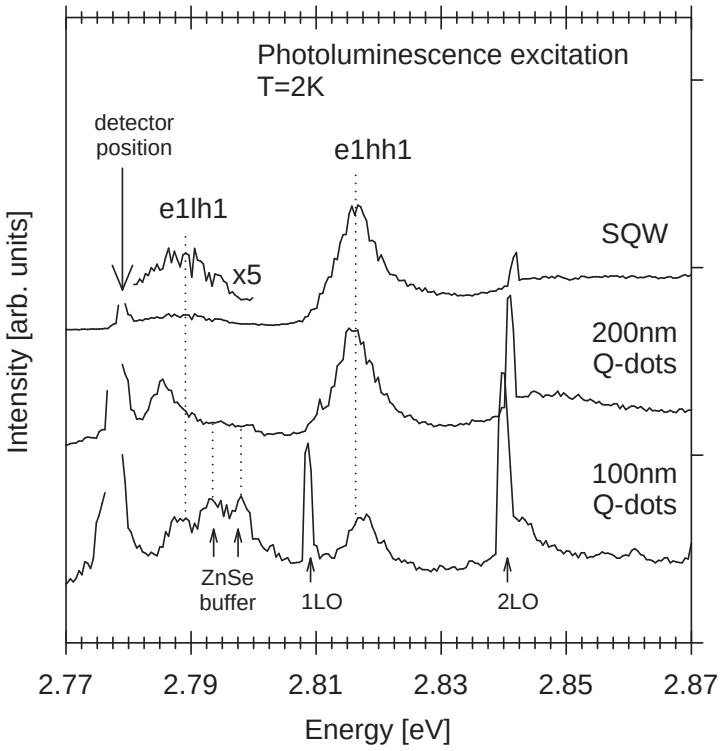

Figure 5: Photoluminescence excitation spectra of the parent $Zn_{0.72}Mn_{0.28}Se/ZnSe$ structure and the 200 nm and 100 nm Q-disc samples. The spectra are shifted vertically for clarity. The quantum well excitonic heavy-hole and light-hole transitions are labelled e1hh1 and e1lh1. Two lines arising from LO phonon Raman scattering are indicated by 1LO and 2LO respectively.

The behaviour of the PLE bands in the case of σ^+ circularly polarised light is more complicated and a detailed discussion is beyond the scope of this paper: briefly, a transition of the band alignment from type-I to type-II leads to the disappearance of the e1hh1 PLE peak at a magnetic field of about 1.5 Tesla.

Let us now compare the excitation spectra (figure 5) of the three specimens at zero field. For the original, unetched layer, two bands are observed that can be attributed to excitonic transitions. The first of these bands, at about 2.815 eV, is assigned to the lowest heavy-hole quantum well exciton (e1hh1), this interpretation being consistent with the strain in the layer (see below). The second band is much broader and much weaker and, because it rests on a broad PLE background, the position of its peak intensity is difficult to determine; nevertheless, it can be assigned to the e1lh1 exciton of the well. In the spectra of the Q-discs, the e1lh1 excitonic bands are sharper and their positions are close

to those of the corresponding emission bands; as in the PL spectra, their peak positions are shifted first towards lower energy (for the 200 nm Q-discs) and then back by about 2 meV (for the 100 nm Q-discs). In contrast, the position of the e1hh1 band remains the same and its width is unaltered; this observation is readily accounted for since the heavy hole exciton transitions are expected to be much less sensitive to strain than are those of the light hole excitons.

For the original SQW layer, when the detection energy for the PLE is changed, the bands attributed to the heavy-hole excitons (e1hh1) remain fixed in energy (as expected). The behaviour of the band attributed to the light-hole exciton (e1lh1) is, however, rather complicated. Firstly, we remark that the intensity of this band relative to that of the heavy-hole band is smaller than expected (the oscillator strengths for the corresponding absorption bands are in the ratio 1:3 and this ratio is approached in the case of the quantum discs). Secondly, the peak position appears not to be independent of the detection wavelength. These observations suggest that the weak signal shown at 2.789 eV in PLE spectrum for the SQW (figure 5) is only part of a broader band. There therefore appears to be a broadening mechanism that affects the light-hole transitions in the SQW which is absent in the quantum discs. As discussed later, we believe this mechanism to be strain-related, so that the heavy-hole transitions would be affected less severely. In the particular case of the 100 nm Q-discs, two additional bands are observed, at 2.793 eV and 2.798 eV, both originating from the ZnSe buffer layer. The assignments of the signals in the PLE spectra are confirmed by their behaviour in a magnetic field (these measurements will be discussed elsewhere).

Before the discussion of the observations made in figures 3 and 5, it is helpful to recall the structure (figure 1) of the initial $Zn_{0.72}Mn_{0.28}Se$/ZnSe SQW sample and that of the Q-disc samples after the nanofabrication. The strain in the SQW is determined by the thicknesses of the different layers that make up the structure. The thicknesses of the ZnSe buffer layer and the lower Zn(Mn)Se barrier ensure that the region of the buffer, barrier and SQW is relaxed relative to the GaAs substrate, the SQW region itself being strained to a lattice constant intermediate between that of ZnSe and Zn(Mn)Se. Since the Zn(Mn)Se lattice constant is slightly greater than that of ZnSe, the SQW is therefore subjected to biaxial tensile strain, to which a further contribution is made as a result of the differential thermal contraction that occurs between the GaAs substrate and the ZnSe and Zn(Mn)Se layers when the specimen is cooled. These strain effects, together with the effects of the quantum confinement in the well of thickness 5.1 nm, determine the energies of the excitonic transitions in the well region of the unetched structure.

When the quantum well structure is etched to form the pillars, the strain will change as elastic relaxation occurs. Since the $Zn_{0.72}Mn_{0.28}Se$ has a greater lattice constant than the ZnSe and since the quantity of $Zn_{0.72}Mn_{0.28}Se$ in the pillar greatly exceeds that of the ZnSe, the tensile strain in the quantum well is expected to increase when the discs are formed. Such an increase in tensile strain displaces the D^0X and X_{e1lh1} lines to lower energies, as shown in the central spectra of figures 3 and 5.

This shift of the D^0X and X_{e1lh1} lines would be expected at first sight to become even larger as the disc radius is further decreased. Experimentally, this is clearly not the case and this suggests that when the disc diameter becomes too small, a further elastic relaxation takes place in which the quantum well is no longer fully constrained to the lattice constant of the (much thicker) barrier. For thin layers in free-standing Q-wire structures, such relaxation effects have recently been calculated and compared with experimental observations by Niquet et al. [10], who find that for aspect ratios of wire width to well width of less than ten, significant relaxation of the strain occurs in the regions of the well. In the case of quantum wells in pillar structures of the form studied in the present paper, relaxation of the strain in the well would be expected to occur at larger aspect ratios than for wires. In the 100 nm discs, the aspect ratio is of the order of 20 (see figure 1) and the experimentally observed relation is therefore entirely reasonable.

With decreasing disc size we observe a reduction of the PL linewidths. In the quantum well PL emissions of the 200 nm Q-discs and of the 100 nm Q-discs the D^0X and X_{e1lh1} bands are resolved, whereas for the SQW sample they overlap. There are three explanations for this effect that can be considered. The first is that the broadening in the original layer is due to fluctuations in the alloy composition of the barrier material (a similar broadening has been observed recently in single $In_{1-x}Ga_xAs/GaAs$ quantum discs and has been explained by fluctuations in alloy composition of the well [11]): however, this mechanism can be excluded in the present case, since, for a laser spot of about $1\,mm^2$, we probe simultaneously more than six million discs, in which a distribution of alloy concentrations would still be present. A second explanation is that the linewidth in the original SQW is due to fluctuations in the well width: again, this mechanism can be excluded since such fluctuations would remain after the formation of the discs.

The third explanation (and the one that we favour) is that the linewidth in the original SQW is determined mainly by the strain fields associated with dislocations. To quantify this explanation, we shall assume a typical value for the dislocation density of $10^7\,cm^{-2}$, as observed in similar samples [12] (implying a mean separation of $3 \cdot 10^4$ Å). At a distance r from a dislocation, the strain due to it may be estimated by $b/(2\pi r)$, where b is the Burgers vector for the dislocation. The implications of this for the PL linewidth before nanofabrication can be seen by noting that the X_{e1lh1} exciton in ZnSe shifts in energy by 4 meV for a change in strain of 0.5 % [13]. If, for the purposes of a simple estimate, we consider regions of the layer as unaffected by a dislocation when the local X_{e1lh1} energy is shifted by less than 0.1 meV then a value of r may be found which defines the boundary separating the regions affected and unaffected by that dislocation (around 7000 Å). Comparing the area of affected regions with the mean area per dislocation (of $9 \cdot 10^8$ Å^2) shows that in about 20 % of the epilayer, the light hole exciton energy is shifted by at least 0.1 meV due to the presence of the dislocation-related strain fields. The broadening of the X_{e1lh1} emission is therefore expected to be significant before nanofabrication. When discs are formed by etching, the probability of a given disc containing a dislocation is,

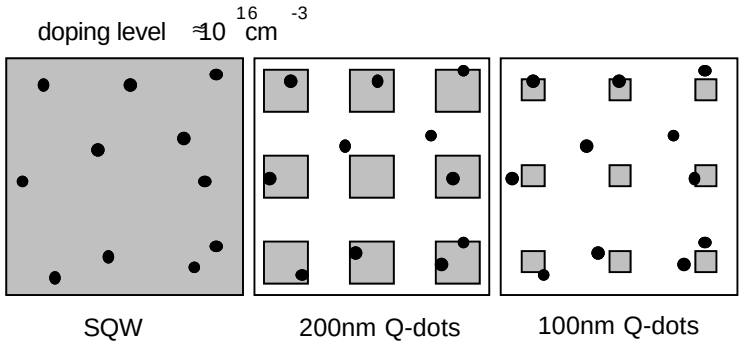

Figure 6: Illustration of the increase of the number of quantum discs without donor ions in the quantum well layer with decreasing disc radius. The black circles represent the donor ions and the grey areas represent schematically the remaining quantum well layer after etching in the three specimens. Note that the diagram is drawn approximately to scale.

even for a diameter of 200 nm, very small (for a dislocation density of $10^7\,\mathrm{cm}^{-2}$ the probability is less than 1 %). Under these assumptions, the quantum discs would therefore be expected to be uniformly in the same strain state, giving rise to the observed narrowing of the light-hole excitonic bands in the optical spectra (the heavy-hole lines are already narrow since they are less sensitive to strain and are not affected significantly in this way).

The observation that the intensity of the PL emission of the bound exciton D^0X decreases more strongly than the free exciton emission X_{e1lh1} with decreasing Q-disc size is, at first sight, unexpected, but can be accounted for by a similar size-related argument, as depicted schematically in figure 6. The SQW sample is unintentionally doped n-type with an upper limit of the doping level being $10^{16}\,\mathrm{cm}^{-3}$. If the ZnSe quantum well region of a Q-disc of diameter d is approximated by a box of $5\,\mathrm{nm} \times d \times d$, a doping level of $10^{16}\,\mathrm{cm}^{-3}$ results in an average of 2 donor ions per ZnSe well in a 200 nm Q-disc and of 0.5 donor ions per ZnSe well in a 100 nm Q-disc. Statistically, the number of Q-discs without donor ions in the ZnSe well increases with decreasing Q-disc size. For this argument to hold, it is essential that, in the ZnSe quantum well of the unetched sample, the cross-sectional areas of the donor ions for exciton capture overlap or, at least, that the cross-sectional area for exciton capture of an individual donor ion is bigger than the lateral dimension of the Q-discs in the etched specimen i e. bigger than 100 nm to 200 nm. Most of the photo-created excitons in the unetched specimen will then reach a donor ion before they decay radiatively. The mean distance between donors is about 450 nm for a density of $10^{16}\,\mathrm{cm}^{-3}$. Most of the excitons which contribute to the quantum well PL emission are created in the $Zn_{0.72}Mn_{0.28}Se$ barriers and migrate to the ZnSe well. These excitons therefore have a non-zero momentum and can travel long distances in the quantum well before they decay radiatively. Thus, the decrease of the bound exciton emission D^0X relative to the free exciton emission X_{e1lh1}

can be consistently explained by an increase of the number of Q-discs without donor ions in the ZnSe well region with decreasing Q-disc size and can be considered as a genuine size effect.

4 Conclusions

The combination of Ar^{2+} ion beam etching and wet-chemical etching offers a promising way for the fabrication of good quality quantum disc structures with high pattern densities. The optical studies of the two quantum disc samples (100 nm and 200 nm in diameter) prepared by this method and of their $Zn_{0.72}Mn_{0.28}Se$/ZnSe SQW parent structure reveal a line-narrowing of the light-hole excitonic bands in both the PL and PLE spectra, together with an enhancement of the intensity of the free exciton relative to the donor-bound exciton in the quantum discs. Both these observations are a consequence of the small lateral size of the discs but are not related to quantum confinement in the plane of the disc. The shifts in the positions of the light-hole exciton lines are related to elastic relaxation that occurs during the formation of the pillars and suggest that pillars 100 nm in height and with a diameter of 200 nm are already small enough to behave as free-standing structures but that when the ratio of disc radius to pillar height becomes too small, further relaxation occurs, as pointed out for quantum wire structures [10]. Because of the size effect that results in the probability of a dislocation being present in a given pillar being very small, all quantum discs are relaxed to a similar strain state. An important aspect of the work is the insight into effects of nanofabrication that can be gained by studying structures in an intermediate size regime before the additional effects caused by lateral quantum confinement complicate the behaviour. The knowledge gained by the study of quantum discs is therefore an important step towards the understanding of structures in which additional lateral confinement effects do indeed arise.

Acknowledgements

We gratefully acknowledge the financial support of the British Council, Deutscher Akademischer Austauschdienst and of the Engineering and Physical Sciences Research Council (GR/K04859). PJK thanks the University of East Anglia for a research studentship. We also thank N. Hoffmann and J. Griesche for the growth of the SQW sample from which the discs were fabricated.

References

[1] L. S. Dang, C. Gourgon, N. Magnea, H. Mariette and C. Vieu, Semicond. Sci. Technol. **9**, 1953 (1994)

[2] P. J. Klar, D. Wolverson, D. E. Ashenford, B. Lunn and T. Henning, Semicond. Sci. Technol. **11**, 1863 (1996)

[3] M. A. Foad, C. D. W. Wilkinson, C. Dunscomb and R. H. Williams, Appl. Phys. Lett. **60**, 2531 (1992)

[4] G. Bacher, M. Illing, A. Forchel, D. Hommel, B. Jobst and G. Landwehr, phys. stat. sol.(b) **187**, 371 (1995)

[5] M. Illing, G. Bacher, T. Kümmell, A. Forchel, T. G. Andersson, D. Hommel, B. Jobst and G. Landwehr, Appl. Phys. Lett. **67**, 124 (1995)

[6] S. A. Gurevich, O. A. Lavrona, N. V. Lomasov, S. I. Netserov, V. I. Skopina, E. M. Tanklevskaya, V. V. Travnikov, A. Osinsky, Y. Qiu, H. Temkin, M. Rabe and F. Henneberger, to be published in Electronic Letters (1997)

[7] C. Gourgon, L. S. Dang, H. Mariette, C. Vieu and F. Muller, Appl. Phys. Lett. **66**, 1635 (1995)

[8] P. J. Klar, D. Wolverson, J. J. Davies, B. Lunn, D. E. Ashenford and T. Henning , 23rd Int. Conf. on the Physics of Semiconductors, eds. M Scheffler and R Zimmermann, vol. 2 1485 (World Scientific, 1996)

[9] J. Griesche, N. Hoffmann and K. Jacobs, J. Cryst. Growth **138**, 59 (1994)

[10] Y. M. Niquet, C. Priester and H. Mariette, Phys. Rev. B **55**, R7387 (1997)

[11] R. Steffen, A. Forchel, T. L. Reinecke, T. Koch, M. Albrecht, J. Oshinowo and F. Faller, Phys. Rev. B **54**, 1510 (1996)

[12] Z. H. Yu, S. L. Buczkowski, N. C. Giles and T. H. Myers, Appl. Phys. Letts. **69**, 82 (1996)

[13] H. Mayer, U. Rössler, K. Wolf, A. Elstner, H. Stanzl, T. Reisinger and W. Gebhardt, Phys. Rev. B **52**, 4956 (1995)